Preprints (www.preprints.org) | NOT PEER-REVIEWED | Posted: 27 March 2019

sensors

MDPI

Article

Field Effect Transistor Anomalous Correlations in odd-even chain parity

Jorsi J. da C. Cunha[1,2], Miraci S. Costa[1], Antonio T. M. Beirão[3], Carlos A. B. da Silva Jr[4], Shirsley S. da Silva[4], and Jordan D. Nero[1,5]

[1] *Programa de Pós-Graduação em Física, Universidade Federal do Pará, Belém, 66075-110, Brazil;* jorsicunha@ufpa.br, miraci@ufpa.br, jordan@ufpa.br

[2] *Faculdade de Matemática, Universidade Federal do Pará, Breves, 68800-000, Brazil*; jorsicunha@ufpa.br

[3] *Campus de Parauapebas, Universidade Federal Rural da Amazônia, Parauapebas, 68515-000, Brazil*; thiago.ppgee.ufpa@gmail.com

[4] *Faculdade de Física, Universidade Federal do Pará, Ananindeua, 67113-901, Brazil*; cabsjr@ufpa.br, shirsleys@gmail.com

[5] *Faculdade de Física, Universidade Federal do Pará, Belém, 66075-110, Brazil*; jordan@ufpa.br

* Correspondence: cabsjr@ufpa.br; Tel.: + 55-91-3201-7423

Abstract: The electronic transport stability in nanodevices composed by metal/trans-polyacetylene /metal with different long length has contributed greatly for performance, homogeneity, stability, organization of the chains, reproducibility and higher conductivity. In this paper, we present an analytical study of the electronic transport characteristics from dimerized trans-polyacetylene (trans-PA) molecules containing an odd-even number of sites coupled to metal leads (left and right) in T-shaped geometry using the extended Su-Schrieffer-Heeger (SSH) model based on tight-binding Hamiltonian with the Non-Equilibrium Green´s Function (NEGF) via Heisenberg´s equation of motion and the Keldysh´s formalism. Due to the complexity of the T-shaped odd-even chain, our proposal was to test the effects on the finite-length network for three, four, five sites and furthermore foresee for 17-sites. We show how to tune dimerization strength (δ) coupling to the parameters and T-shaped geometry of the device to which it affects the overlap integral localized at the three endpoints of the T-shaped system, making both the odd and even chains to undergo a metal-insulator transition in their electronic behavior. The results reached through control parity of the chain plane of the parameters governing (δ) the electronic and experimental tunneling allow a better understanding of the subject.

Keywords: Anomalous; correlations; trans-PA; electronic transport; FET.

1. Introduction

Low dimensionality systems, such as conjugated polymers, have been extensively investigated, allowing the study of fundamental aspects of quantum mechanics and interactions between individual donor-bridge-receptor molecules [1]. Studies have shown that conjugated polymers can be conductor or semiconductor when doped [2]. Polyacetylene (PA) is the simplest conjugated polymer, which has electrical conductivity close to that of semiconductors such as silicon [3], whose properties could be investigated using Hamiltonians based on simple models [4,5]. Important advance have been made in theoretical modeling of electronic transport when the donor and/or acceptor group is replaced by metal or semiconductor electrodes, i. e., when metal/polymer/metal junctions are characterized by several research groups [6-9], to investigate the dependence on the bridge structure and the electronic properties of the bonds [10]. In this process, the

© 2019 by the author(s). Distributed under a Creative Commons CC BY license.

Preprints (www.preprints.org) | NOT PEER-REVIEWED | Posted: 27 March 2019

metal-molecule-metal coupling depends on many parameters, such as the type of chemical bond between them, the molecular conformation and the height of the tunneling barrier [11, 12].

Recently, we have investigated the properties of electronic transport through analytical calculations of the Green´s function of a T-shaped semiconductor nanostructure junction, where one single-level quantum dot (QD) is coupled to two Leads (Left and Right) and a Carbon nanowire with triangular zigzag geometry formed by two Kitaev chains (with odd or even number of sites) above a topological superconductor with p-wave pairing to which it for proximity effect Majorana zero modes can be tuned through the coupling factor of the device. The linear conductance shows *Majorana bound states* (MBS) in the topological phase, being maximally robust in the general topological phase [13].

Thus, we propose to investigate the electronic transport properties using the modified Tight-Binding model, with alternation of single and double bonds, proposed by Su, Schrieffer and Heeger (SSH) [14], or SSH model, which addresses specific properties of conducting polymers [15] approaching a real chain by a finite number of sites with periodic boundary conditions, making the SSH model of PA chains a non-rotating 1-D symmetric tight-binding model extensively studied with alternating hopping constants [16].

In this paper the two topologically different phase and different dimerizations strengths (δ) can generate zero-energy states. We find in SSH model nontrivial topology through opposite odd-even parity of the number of sites due differents δ. Disorders effects can be observed in density states (DOS) because of de size of the chain, since as the disorder increases the states become more located (Anderson transition) [17], in addition to electron-electron influence on the system (Mott transition) [18-20]. Highilighting the possible quantum effects with located with state transitions delocalized-located [21]. Experimentally is relevant the study finite-length chains. Once that the long semiconductor nanowire device are considered segmented by disorder in a smaller number of coherent chains [22]. We investigated T-shaped epolyacetilene nanowire focusing in your finite size and effects of the electronic transport due no trivial effects in odd-even chain.

Figure 1 shows the system to be investigated composed of trans-PA molecules covalently bound to two metal Leads (Left and Right), in the T-shaped geometry, where the Leads are coupled to the first site (C_1) that is connected to second site (C_2) and so on, to the site 17 (C_{17}), where the coupling factor between the Leads (Left and Right) and molecule (i. e., Left Lead/molecule/Right Lead) in the devices are given by Γ_L and Γ_R, respectively. The parameter δ is the degree of dimerization and needs to be adjusted to obtain better result of the electronic transport properties.

León *et al*. [23] probed the electronic structure and Au-C chemical bonding using experimental techniques and theoretical results. The Carbon forms covalent bonds with non-metal and metals elements. It shares electrons with atoms/compounds to form a stable structure in nature because it obeys the octet rule. The metal-carbon bonds in organometallic compounds are generally highly covalent. Covalent interactions are directional and depend on orbital overlap leading to different types of covalent bonds. The metal-carbon bonds and non-metal-carbon bonds are extensively investigated in electronic transport and applied to develop devices at the molecular scale [24, 25].

Preprints (www.preprints.org) | NOT PEER-REVIEWED | Posted: 27 March 2019

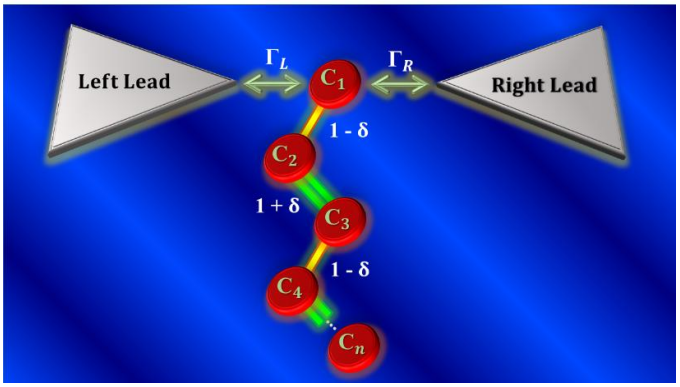

Figure 1. Dimerized trans-PA molecule with *n* sites coupled to the metal leads (Left and Right), where Γ_L and Γ_R are weak couplings of the 1 site (C_1) with the metal contacts, *1-δ* (single bond) and *1+δ* (double bond) represent weak and strong hopping (tunneling), respectively, that depending on the C_1-metal and C-C bond type. In our calculations, we consider the molecule with an even and odd number of sites.

The investigated electronic transport properties are based on analytical calculations using the SSH model [4] combined with the NEGF formalism [26] for the systems of the Figure 1. The equilibrium system use the Heisenberg´s equation of motion, while the nonequilibrium system use the Keldysh formalism based on the retarded, advanced and minor Green´s functions [27-29]. Keldysh's formalism-based approach enables the treatment of electrode-molecule-electrode interactions in a self-consistent manner and works well across the bias range of applied interest [30, 31]. The extended SSH model is employed and combined with an adiabatic dynamic method, which has been widely used in the investigation of the dynamics of soliton, polaron and bipolaron [5, 14], besides exploring the inversion of photoinduced polarization [32, 33] in conjugated polymers.

In this way, this paper was divided as follows. Section II, we present the model and methodology through a detailed derivation of the transport equations, where we obtain the Green´s functions, both in: *(i)* Equilibrium to determine the normalized density of states [$DOS(x\pi\Gamma_L)$] and Transmittance [$T(E)$] versus energy [$E(\omega)$]; and *(ii)* NonEquilibrium to determine the current-voltage (I-V) curve, differential conductance-voltage (dI/dV - V) curve and [$(dI/dV)_{max}$ – n]. Section III, we exhibit the main results found. Section IV, we made the final considerations.

2. Model and Methodology

We considered a 1-D chain spinless of the dimerized trans-polyacetylene molecule whose site 1 (C_1) was coupled to metal leads (Left and Right) through a symmetric coupling factor, Γ_L and Γ_R. Equation (1) below shows the Hamiltonian of the system for a model dimerized with each carbon atom interacting with the nearest neighbor,

$$H = H_L + H_{SSH} + H_{LSSH} \tag{1}$$

the first term of the Eq. (1) represents the leads (Left and Right), which can be described by Eq. (2),

Preprints (www.preprints.org) | NOT PEER-REVIEWED | Posted: 27 March 2019

$$H_L = \sum_{k\alpha} \varepsilon_k c_{k\alpha}^{+} c_{k\alpha} \tag{2}$$

where, $c_{k\alpha}^{+}$ ($c_{k\alpha}$) denotes the electrons creation (annihilation) operators [34] on the leads (Left and Right), ε_k represent the leads energy in the momentum **k**.

The term H_{SSH} of the Eq. (1) describes a dimerized trans-PA molecule in the modified SSH model, for a chain containing *n* carbons, which can be written by Eq. (3),

$$H_M = \sum_{i=1}^{n} \left\{ \left[1 + (-1)^i \delta \right] c_i^{+} c_{i+1} + h.c \right\} + h \sum_{i=1}^{N} c_i^{+} c_i \tag{3}$$

where c_i^{+} create electrons in the site *i* and c_{i+1} annihilates such electron in the site *i+1* and *i* represents the number of Carbons in PA chain, i. e., $i = 1, 2, 3, \ldots, n$. The hopping integral (hopping in the same sublattice) between next nearest-neighbor sites is stteped between $A = 1+\delta$ and $B = 1-\delta$, δ is the degree of dimerization. Being 1 the average of the tunneling intensity. To ensure that the probability of displacement along the chain is equal, we consider $|\delta| < 1$. Each unit cell contains two sites belonging to two subnets, designated by Y and Y′ in the SSH model [35]. The parameter *h* represents the chemical potential [36]. The last term H_{LSSH} of the Eq. (1) describes the interaction between the Leads and site 1 that is given by Eq. (4),

$$H_{LSSH} = \sum_{k\alpha} V_{k\alpha} \left(c_{k\alpha}^{+} c_1 + c_1^{+} c_{k\alpha} \right) \tag{4}$$

being $V_{k\alpha}$ the electronic tunneling between the first site and the leads (Left and Right).

Using the recursive method of retarded Green´s functions which describes the configuration indicated in Fig. 1 for the analytical calculations based on the technique of the Heisenberg´s equation of motion. Considering the geometry of the system, we perform the calculations of the Green´s function of the first site, $G_{c_1c_1}^{r}(\omega)$, for i = 1, 2, 3, 4, 5 and 6 carbonsand then we generalize the calculations to an even and odd number of n carbons contained in the chain of the dimerized trans-PA molecule.

For the case, where, *n* is even, we have the set of *Eqs.* (*i*)-(*v*)

$$(\omega - \varepsilon_k) G_{c_{k\alpha}c_1}^{r}(\omega) = V_{k\alpha} G_{c_1c_1}^{r}(\omega) \tag{i}$$

$$(\omega - h) G_{c_nc_1}^{r}(\omega) = A G_{c_{n-1}c_1}^{r}(\omega) \tag{ii}$$

$$(\omega - h) G_{c_{n-1}c_1}^{r}(\omega) = B G_{c_{n-2}c_1}^{r}(\omega) + A G_{c_nc_1}^{r}(\omega) \tag{iii}$$

$$(\omega - h) G_{c_{n-2}c_1}^{r}(\omega) = B G_{c_{n-3}c_1}^{r}(\omega) + A G_{c_{n-1}c_1}^{r}(\omega) \tag{iv}$$

....

$$(\omega - h) G_{c_1c_1}^{r}(\omega) = 1 + B G_{c_2c_1}^{r}(\omega) + V_{k\alpha} G_{c_{k\alpha}c_1}^{r}(\omega) \tag{v}$$

Preprints (www.preprints.org) | NOT PEER-REVIEWED | Posted: 27 March 2019

where *(i)* gives the dynamics of the Leads (Left and Right) and describes the Green´s function of their interaction with site 1, *(ii)* describes the interaction of site *n* with site *n-1*; *(iii)* describes the interaction of site *n-1* with sites *n* and *n-2*, *(iv)* exhibits the interaction of site *n-2* with sites *n-1* and *n-3*, ... *(v)* represents the site 1 dynamics and their interaction with the Leads (Left and Right) and site 2. Replacing *(ii)* in *(iii)*, *(iii)* in *(iv)*, following this reasoning, we arrive at the *(v)* and obtain the recursive formula for the Green´s function of site 1, with *n* sites, where *n* is even, given by Eq. (5).

$$G^r_{c_1c_1}(\omega)=\cfrac{1}{\omega-h-\cfrac{B^2}{\omega-h-\cfrac{A^2}{\omega-h.....\cfrac{B^2}{\omega-h}}}+i\Gamma} \tag{5}$$

Equation (5), the hopping $B = [1+(-1)^{n-1}\delta]$ repeats $\frac{n}{2}$ times and the hopping $A = [1+(-1)^{n}\delta]$ repeats $\frac{n}{2}-1$ times.

For the case where, *n* is odd, we obtain the set of *Eqs.* (*vi-x*)

$$(\omega-\varepsilon_k)G^r_{c_{k\alpha}c_1}(\omega)=V_{k\alpha}G^r_{c_1c_1}(\omega) \tag{vi}$$

$$(\omega-h)G^r_{c_nc_1}(\omega)=BG^r_{c_{n-1}c_1}(\omega) \tag{vii}$$

$$(\omega-h)G^r_{c_{n-1}c_1}(\omega)=AG^r_{c_{n-2}c_1}(\omega)+BG^r_{c_nc_1}(\omega) \tag{viii}$$

$$(\omega-h)G^r_{c_{n-2}c_1}(\omega)=B+AG^r_{c_{n-1}c_1}(\omega) \tag{ix}$$

...

$$(\omega-h)G^r_{c_1c_1}(\omega)=1+BG^r_{c_2c_1}(\omega)+V_{k\alpha}G^r_{c_{k\alpha}c_1}(\omega) \tag{x}$$

Similarly, to the *(i)-(v)*, we describe the *(vi)-(x)* and obtain the recursive formula for the Green´s function of site 1, for *n* sites, where *n* is odd, given by Eq. (6),

$$G^r_{c_1c_1}(\omega)=\cfrac{1}{\omega-h-\cfrac{B^2}{\omega-h-\cfrac{A^2}{\omega-h.....\cfrac{A^2}{\omega-h}}}+i\Gamma} \tag{6}$$

Equation (6), the hoppings $B = [1+(-1)^{n}\delta]$ and $A = [1+(-1)^{n-1}\delta]$ repeats $\frac{n-1}{2}$ times.

The Green´s function of the site 1, $G^r_{c_1c_1}(\omega)$ is important for our results, because it is from this that we obtain the density of states (DOS) to the electronic transport properties, which will be presented in Section III of this paper.

Preprints (www.preprints.org) | NOT PEER-REVIEWED | Posted: 27 March 2019

The previously obtained Green´s functions, $G^{r}_{c_1c_1}(\omega)$, will provide the DOS, $\rho(\omega)$, for 1, 2, 3, 4, 5 and 6 carbons, when combined in Equation, $\rho(\omega)=\left(-\frac{1}{\pi}\right)\mathrm{Im}\left[G^{r}_{c_1c_1}(\omega)\right]$.

Non-Equilibrium situation, we calculate analytically the electronic transport properties, as current and differential conductance of the system versus bias voltage by means of NEGF, using the Keldysh´s formalism [26]. The current from the Left Lead to the polymer chain is given, as usual by Eq. (7) [37]:

$$I_{\alpha}=2e\Re e\left\{\sum_{k\alpha}V_{k\alpha}G^{<}_{c_1k\alpha}(t,t')\right\} \tag{7}$$

where, $G^{<}_{c_1k\alpha}(t,t')=i\left\langle c^{+}_{k\alpha}(t)c_1(t')\right\rangle$. The current flow and can be evaluated by Eq. (8):

$$I_{\alpha}=\frac{e}{2\pi\hbar}\int T(E,V)f(E)dE \tag{8}$$

Where $T(E,V)=Tr\left[\Gamma_L G^{r}_{c_1}\Gamma_R G^{a}_{c_1}\right]$ is the transmittance, $f_{\alpha}=\frac{1}{e^{\frac{\varepsilon-\mu_{\alpha}}{K_BT}}+1}$ is the Fermi distribution function at the Lead chemical potential μ_{α} (α = L (Left) or R (Right)) and the functions $G^{r}_{c_1}$, $G^{a}_{c_1}$ and $G^{<}_{c_1}$ are the Green´s functions (retarded, advanced and minor) for the site 1. As a starting point we obtain by analytical continuation the Green´s function of ordered contour $G^{<}_{c_1k\alpha}(\tau,\tau')=-i\left\langle T_c(\tau)c^{+}(\tau')\right\rangle$ being that T_c orders the operators along the Keldysh´s contour.

We will now calculate the current. For a molecule of *n* sites, taking the time derivative, we obtain the Eq. (9),

$$\left(i\frac{\partial}{\partial t}-h\right)G^{r}_{c_1}(t,t')=\delta(t-t')+\sum_{k\alpha}V_{k\alpha}G^{r}_{k\alpha}(t,t')+BG^{r}_{c_2}(t,t') \tag{9}$$

With $G^{r}_{c_{k\alpha}}(t,t')=-i\left\langle T_c c_{k\alpha}(t)c^{+}_1(t')\right\rangle$ and $G^{r}_{c_2}(t,t')=-i\left\langle T_c c_2(t)c^{+}_1(t')\right\rangle$. Deriving again, we get the Eq. (10),

$$\left(i\frac{\partial}{\partial t}-\varepsilon_k\right)G^{r}_{c_{k\alpha 1}}(t,t')=V_{k\alpha}G^{r}_{c_1}(t,t') \tag{10}$$

and the Eq. (11),

$$\left(i\frac{\partial}{\partial t}-h\right)G^{r}_{c_2}(t,t')=BG^{r}_{c_1}(t,t')+AG^{r}_{c_3}(t,t') \tag{11}$$

where, $G^{r}_{c_3}(t,t')=-i\left\langle T_c c_3(t)c^{+}_1(t')\right\rangle$ that deriving we obtain the Eq. (12),

Preprints (www.preprints.org) | NOT PEER-REVIEWED | Posted: 27 March 2019

$$\left(i\frac{\partial}{\partial t}-h\right)G^r_{c_3}(t,t')=AG^r_{c_2}(t,t')+BG^r_{c_4}(t,t') \tag{12}$$

Following this reasoning, we arrive at the Eq. (13),

$$\left(i\frac{\partial}{\partial t}-h\right)G^r_{c_n}(t,t')=AG^r_{c_{n-1}}(t,t') \tag{13}$$

The *Equations* (9)-(13) constitute a complete set of $n + 1$ differential equations describing the interactions between the Leads with the first site (C_1) and between the neighboring sites (C_n), see Fig. 1. In order to reduce the system to n equations, let's write the Eq. (10) in integral form, we get the Eq. (14),

$$G^r_{k\alpha}(t,t')=V_{k\alpha}\int dt_1 g_{k\alpha}(t,t')V_{k\alpha}(t_1,t') \tag{14}$$

Replacing the Eq. (14) in the Eq. (9), we obtain the Eq. (15),

$$\left(i\frac{\partial}{\partial t}-h\right)G^r_{c_1}(t,t')=\delta(t-t')+\int dt_1\sum(t,t_1)G^r_{c_1}(t,t')+BG^r_{c_2}(t,t') \tag{15}$$

with $\sum(t,t_1)=\sum_{k\alpha}g_{k\alpha}(t,t_1)|V_{k\alpha}|^2$, in a matrix notation they are given by Eq. (16),

$$\vec{G}(t,t')=g(t,t')\vec{u}+\int\int dt_2dt_1g(t,t_2)\sum'(t_2,t_1)\vec{G}(t_1,t') \tag{16}$$

Using the Eq. (16), we obtain the Dyson´s Equation for the system,

$$G(t,t')=g(t,t')+\int\int dt_2dt_1g(t,t_1)\sum'(t_1,t_2)G(t_2,t') \tag{17}$$

Because of the time-convolution integrals in the above equations, it is useful to write down the equations for the Fourier transforms of the Green´s functions. So, in the Keldysh´s contour [37] we have the Eq. (18),

$$G^r(\tau,\tau')=g^r(\tau,\tau')+\iint d\tau_2d\tau_1g(\tau,\tau_1)\tilde{\Sigma}(\tau_1,\tau_2)G(\tau_2,\tau') \tag{18}$$

So, we apply the Langreth´s analytical continuation in (18), we obtain the retarded Green´s function given by Eq. (19),

$$G^r(\omega)=g^r(\omega)+g^r(\omega)\tilde{\Sigma}^r(\omega)G^r(\omega) \tag{19}$$

and for the minor Green´s function, we have the Eq. (20)

$$G^<(\omega)=G^r(\omega)+\tilde{\Sigma}^<(\omega)G^a(\omega) \tag{20}$$

the equations obtained for retarded/advanced/minor Green´s functions are not independent. They form a set of dependent integral-differential equations in the real-time representation or a set of matrix equations in the energy representation. Note that all the above equations for the three real-time Green´s functions are exact and general in the meaning of the perturbation expansion, that is, when one can define self-energies [38].

From where we obtain the components of retarded and minor self-energy given by Eq. (21)

Preprints (www.preprints.org) | NOT PEER-REVIEWED | Posted: 27 March 2019

$$\tilde{\sum}^{<}_{11}(\omega)=\begin{bmatrix} -\frac{i}{2}\Gamma(\omega) & B & 0 & 0 & \cdots & 0 \\ B & 0 & A & 0 & \cdots & 0 \\ 0 & A & 0 & B & \cdots & 0 \\ 0 & 0 & B & 0 & \cdots & 0 \\ \cdots & \cdots & \cdots & \cdots & \cdots & \cdots \\ 0 & 0 & 0 & 0 & \cdots & 0 \end{bmatrix} \tag{21}$$

and the matrix $\tilde{\sum}^{<}(\omega)$ that has only one element different of zero in the Eq. (22),

$$\tilde{\sum}^{<}_{11}(\omega)=i\left[\Gamma_L(\omega)f_L(\omega)+\Gamma_R(\omega)f_R(\omega)\right] \tag{22}$$

Like the other elements from $\tilde{\sum}^{<}(\omega)$ are equal to zero. Self-energies are complex functions of Green's functions and have interesting physical meaning, the real part causes a shift in the self-values, while the imaginary part is responsible for the lifetime of the state, in the space of energies, this process produces a widening of the DOS, where $\Gamma_{L/R}$ is the tunneling rate between the *ith* molecular level and the leads (left and right). Therefore, with the Eqs. (19) and (20) we can to calculate the current of the system through of the Eq. (8) replacing in $T(E,V)=Tr\left[\Gamma_L G^r_{c_1}\Gamma_R G^a_{c_1}\right]$ as well as the differential conductance deriving the current in relation to the voltage.

3. Results and Analysis

Figure 2 exhibit the results of the analytical calculations for the (a) DOS and (b) Transmission Spectrum (or Transmittance) of the metal/trans-PA/metal system composed by trans-PA chains with $n = 3, 5, 7$ *and* 9 sites. We developed calculations at the thermodynamic limit in the context of Green's functions [39, 40]. In this case, the equilibrium to which it considers the symmetric coupling, $\Gamma = \Gamma_L = \Gamma_R$ and the parameters used are: $h = 0eV$ to adjust the DOS and Transmittance peaks with the Fermi level; $\delta = 0.1eV$ denotes the dimerization strength and $\Gamma = 0.5eV$ to keep strong the coupling between the Leads (Left and Right) and chain (molecule).

Figure 2(a) shows the DOS and we identify the energy peaks at the Fermi level, $\omega = 0$. This occurs due to geometry of the system, once for an odd number of sites the chain dimerization is complete, this fact of dimerization besides improving the tunneling in the neighboring carbon atoms, fills the energy space at the Fermi level [41]. In Fig. 2(b), this performance provides a metallic character to the system. Odewise fact, the transmittance decreases with increasing the chain [42].

Preprints (www.preprints.org) | NOT PEER-REVIEWED | Posted: 27 March 2019

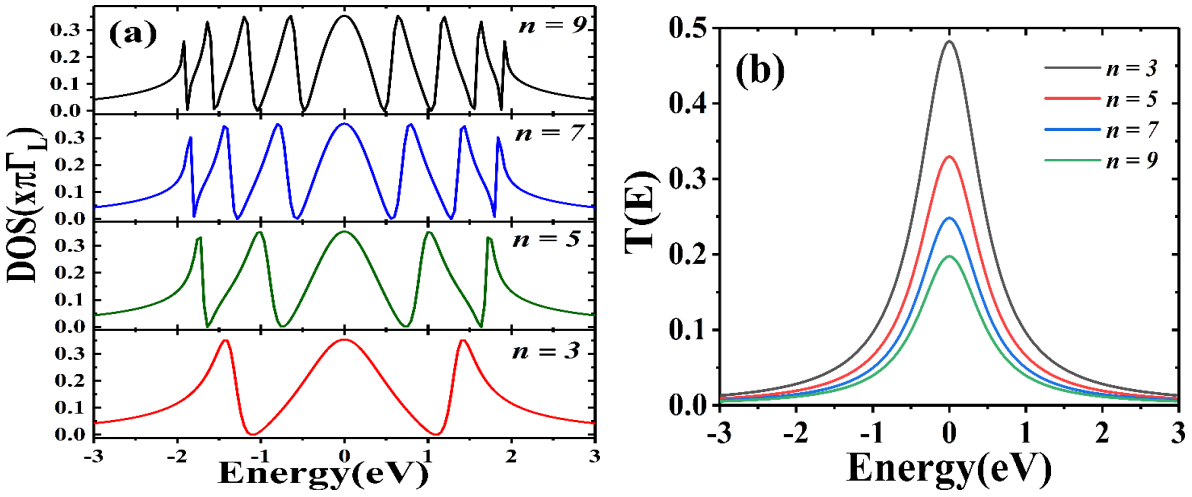

Figure 2. DOS and Transmittance [T(E)] versus Energy for the metal/trans-PA/metal system with the coupling parameters $\Gamma_L = \Gamma_R = 0.5eV$; hopping between neighboring sites, in the same subnet, $A = 1+\delta$ and $B = 1-\delta$ where $\delta = 0.1eV$; and chemical potential, $h = 0eV$. **(a)** DOS for odd chains (3, 5, 7 and 9 sites represented by red, green, blue and black lines, respectively) and **(b)** Transmittance for odds chains (3, 5, 7 and 9 sites represented by black, red, blue and green lines, respectively).

Figure 3 exhibits the electronic transport properties by means of the (a) *I-V* and (b) *dI/dV-V* curves, whose parameters are $\Gamma = 0.5eV$ and $\delta = 0.1eV$ for odd chains, $3 \leq n \leq 17$ sites. The effect of an applied external voltage is from the shifting of the chemical potentials of the two Leads (μ_L and μ_R) relative to each other by eV, where e is the electronic charge. It´s observed in the Fig. 3(a), the non-linear (or non-ohmic) behavior of the *I-V* curve which is symmetrically manifested in both bias (direct and reverse) and that these systems possess characteristic of electronic and optoelectronic devices such as *Field Effect Transistor* (FET). However, the current presents a metallic behavior between $0.0V \leq V \leq 0.5V$ (inset in Fig. 3a) due to the linear character of the *I-V* curve in this interval and a change in the conduction regime is observed between $0.6V \leq V \leq 2.0V$ presenting a resonance region. After $2.0V$ the *I-V* curve tends to a region of saturation. Figure 3(b) exhibits the *dI/dV-V* curve ($G = dI/dV$ = conductance) which the conductance is maximum for zero bias and is nearly invariant for bias voltage up to $0.5V$ (inset in Fig. 3b) and decrease considering the resonant tunneling model for $K_B.T = 0.026eV/K$, where $K_B = 0.00008617eV$ and $T = 300K$.

The chains with odd number of sites exhibit common fermions (electrons) at ε_F and FET behavior in *I-V* curve due the resulting dimerization from the Peierls distortion which characterize a metal-insulator transition due to the opening of gaps.

Preprints (www.preprints.org) | NOT PEER-REVIEWED | Posted: 27 March 2019

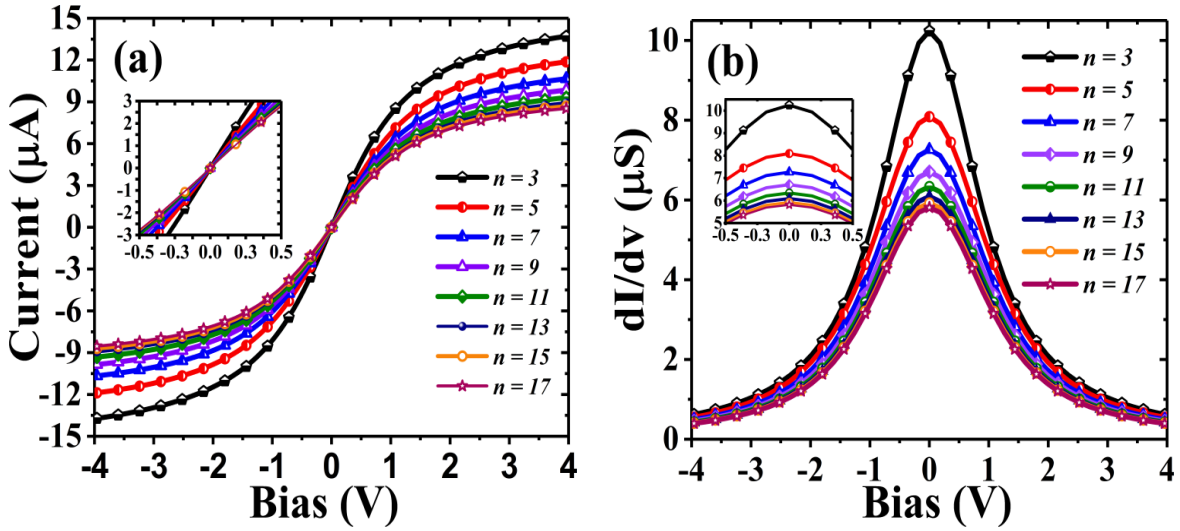

Figure 3. Characteristic curves of the transport properties for chains with odd numbers of sites (3, 5, 7, 9, 11, 13, 15 and 17 sites) coupled to the Leads (Left and Right) with the paramers $\Gamma = 0.5eV$, hoppings $A = 1+\delta$ and $B = 1-\delta$, $\delta = 0.1eV$. **(a)** *I-V* curve with voltage from -4V to 4V, characterizing FET, in the insert Fig. 3(a) we have the current for low voltages assume metallic behavior and **(b)** curves of differential conductance versus voltage, highlighting the resonance peaks in the inset Fig. 3(b).

We can control the electronic tune through different dimerization strength (δ) of chain and analyze for all driving windows $-4.0eV$ to $4.0eV$. For a molecule with five sites (i. e., $n = 5$), see Fig. 4(a) represents the behavior of the current for four values of the dimerization strength (δ) in hoppings $A = 1+\delta$ and $B = 1-\delta$, respectively, where we adopt: $\delta = 0.01eV$, $\delta = 0.1eV$, $\delta = 0.5eV$ and $\delta = 0.8eV$. We take into account the parameter $|\delta| < 1$ where 1 is the maximum tunneling for the intracell-to-intercell coupling in the chain [6, 7, 12]. Figure 4(a) confirms the FET behavior for the device investigated. On the other hand, Fig. 4(a) shows anomalous effects related to the uniform chain geometry. For the dimer chain $\delta = 0.5eV$ (yellow line with triangle down) and $\delta = 0.8eV$ (blue line with triangle up), the tunneling is approximately equal. The polymer chain becomes more dimer, affecting the conductivity. Such a condition can be interpreted as structural and conformational defects that generally reduce the superposition of π states, acting as localizer centers that interrupt conjugation along the polymer chain. According to previous studies in the literature, as an example in Oliveira *et al*. [43] this reports a semiconductor PA chain that exhibits nonlinear behavior for *I-V* curve at low and high voltage. Or negative differential resistance (NDR) effect, they could occur in greater bias due to a displacement of the conduction channels in relation to the electronic states of the contact Leads under external bias [44, 45].

Preprints (www.preprints.org) | NOT PEER-REVIEWED | Posted: 27 March 2019

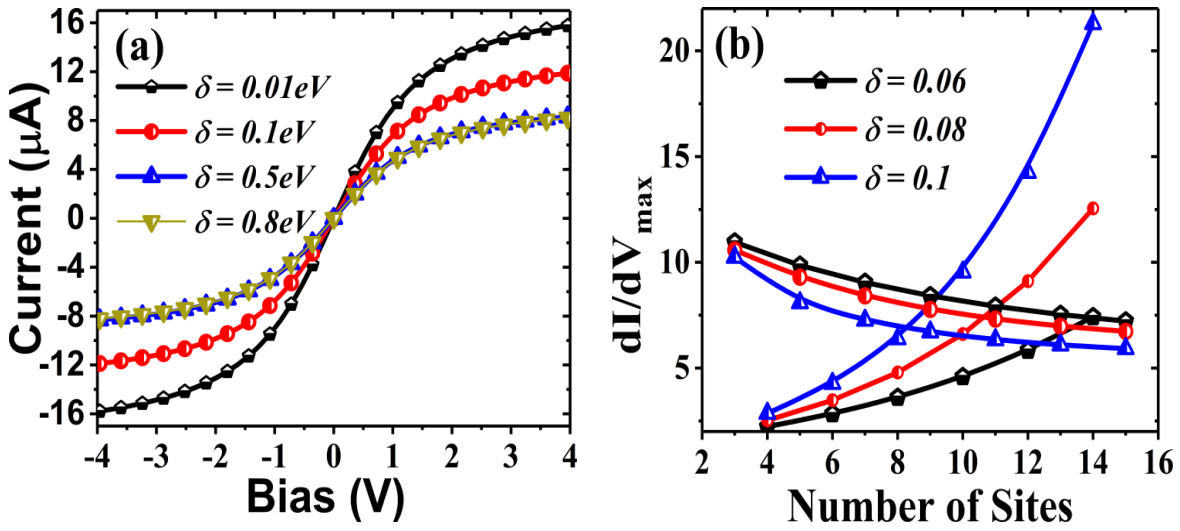

Figure 4. (a) *I-V* curve for one chain with five (n = 5) sites considering four values differents for the parameter δ: (1) *0.01eV* (open trapeze, black color); (2) *0.1eV* (open ball, red color); (3) *0.5eV* (open triangle, blue color); and (4) *0.8eV* (open triangle, yellow color), keeping $\Gamma = 0.5eV$. **(b)** keeping $\Gamma = 0.5eV$ and varying δ, i. e, *0.06eV* (open trapeze, black color), *0.08eV* (open ball, red color) and *0.1eV* (pentagon semi-closed, blue color).

Figure 4 (a) confirms the behavior of Fig. 4 (b) increasing the dimerization effect (δ) in the chain reduces the maximum conductance $[dI/dV]_{max}$ to the odd number of sites. But, the reverse process occurs in the chain with even number of sites besides is exhibited the points of intersection at approximately *n = 14*, *11* and *8* for δ = 0.06eV, 0.08eV and 0.1eV respectively between the odd and even functions. We have showing an opposite odd-even parity. For instance, the dimer chain with δ = 0.06eV has a perfect transmission only even chain, whereas it as perfect reflection for only odd chain.

In order to design PA chain based T-shaped device, we exhibit the Fig. 5(a) for chains with *n = 4*, *6*, *8* and *10* which starts and ends with the hopping $B = [1+(-1)^{n-1}\delta]$ increasing the tunneling barrier, creating an energy gap opens up at the Fermi level of the polymer. These results can be explained in an analytical way with the help of Eqs. (5) and (6). It is clearly seen that in the zero-energy limit, the Green´s function of the site *n = 1*, $G^{r}_{c_1c_1}(\omega)$ has only two values. The chains with even number of sites not exhibit common fermions (electrons) at ε_F for the DOS. The transmittance in the Fig. 5(b) for even chains have a tail, since in this case the wide bias window and the Fermi level are close to conduction region band [46].

Preprints (www.preprints.org) | NOT PEER-REVIEWED | Posted: 27 March 2019

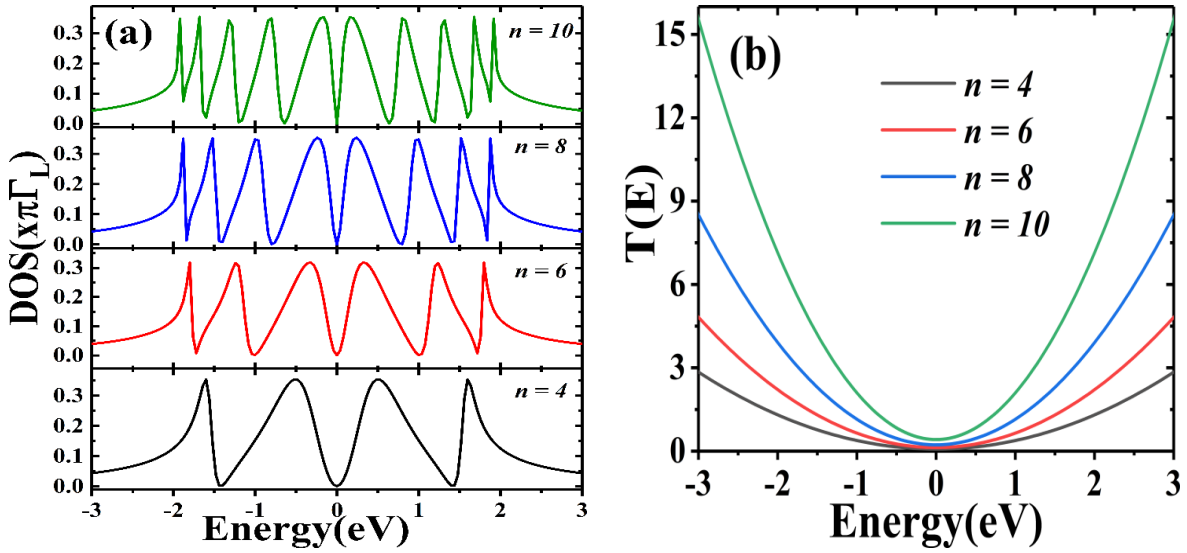

Figure 5. (a) DOS and **(b)** Transmittance [T(E)] versus Energy for the metal/trans-PA/metal system with the coupling parameters $\Gamma_L = \Gamma_R = 0.5eV$; hopping between neighboring sites, in the same subnet, $A = 1+\delta$ and $B = 1-\delta$ where $\delta = 0.1eV$; and chemical potential, $h = 0eV$ **(a)** DOS for even chains (4, 6, 8 and 10 sites) represented by black, red, blue and green lines, respectively) and **(b)** Transmittance for odds chains. (4, 6, 8 and 10 sites) represented in the same DOS colors.

The *I-V* characteristics for even chains (i. e., $n = 4, 6, 8$ and 10) have been summarized in Fig. 6 by *ln(I)-V* curve and shows quasi-ohmic region up to $0.5V$. When the chain number of sites increases by $n = 4$ up to $n = 10$ sites, the ln(I)–V curve through the junction increases very slowly and the up inclination in the *ln(I)-V* curve is due to the difference in the resistances as offered. For even chains, Fermi level was near the valence and the conduction resonance peak, which helps in electron transport, as shown the Fig. 5 (a). For the conduction region, its behavior has an "electron-acceptor" character as consequence the smaller its energy, the smaller the resistance [44].

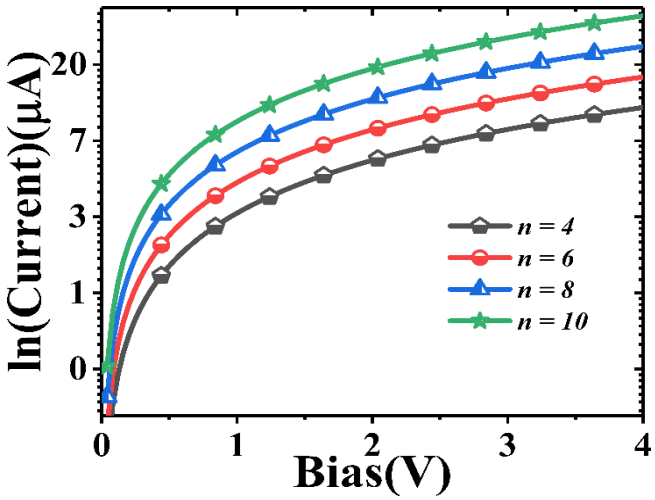

Figure 6. Transport characteristic (ln of the current) from the system coupled to the Leads (Left and Right) to the even chains, (4, 6, 8 and 10 sites) with the paramers $\Gamma = 0.5eV$, hoppings $A = 1+\delta$ and $B = 1-\delta$, with $\delta = 0.1$eV.

Preprints (www.preprints.org) | NOT PEER-REVIEWED | Posted: 27 March 2019

If we derive the *ln(I)* with respect to voltage, i. e., *dln(I)/dV* curve can to obtain the Fig 7(a-d) for the even chains (n = *n* = *4*, *6*, *8* and *10*). The peaks respectively, are due to the stepwise increase of excitation states available on the chain as tunneling paths. This intrinsic noise allows us to obtain information about the dynamics of carriers. As partial oscillations, they were found in the C, Na and Si chains. This effect was experimentally confirmed for the Au, Pt and Ir wires through the junction of a control bridge mechanically [47].

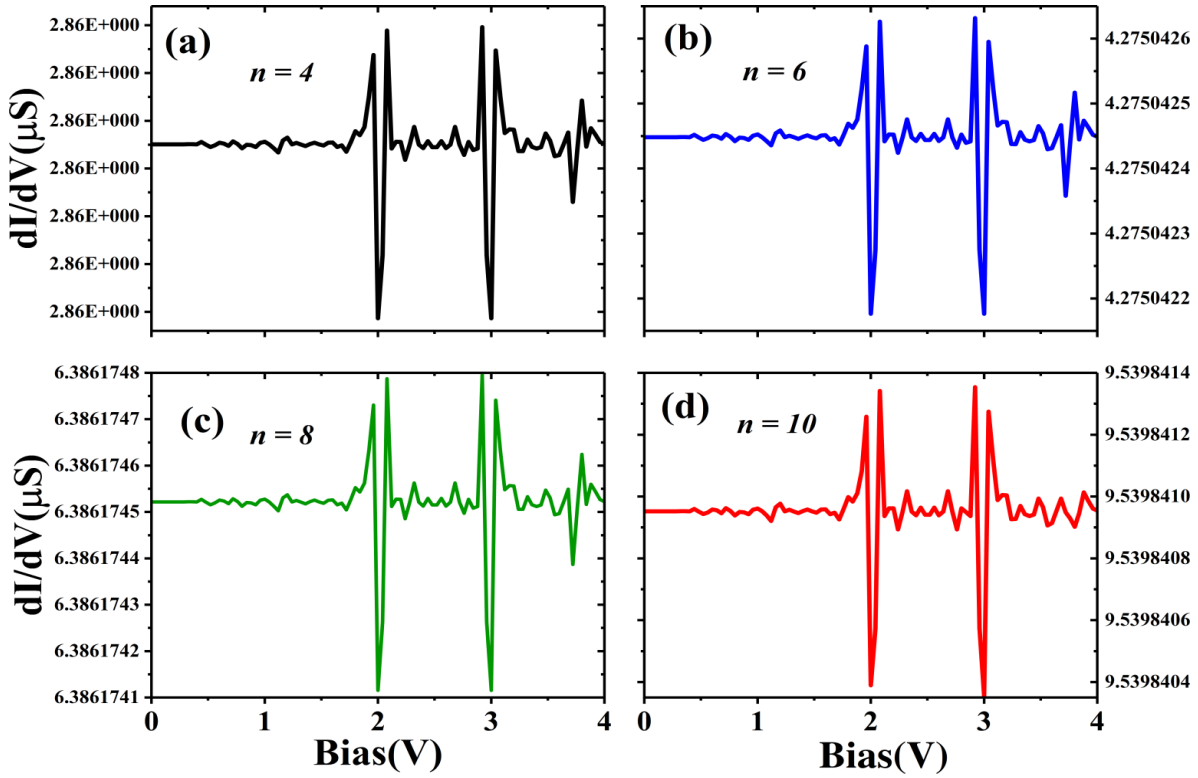

Figure 7- Electronic transport properties (Differential Conductivity) of the system for the even chains (4, 6, 8 and 10 sites) with the paramers $\Gamma = 0.5eV$, hoppings $A = 1+\delta$ and $B = 1-\delta$, $\delta = 0.1$eV for an applied external voltage of *0.0eV* to *4.0eV*. The dln(I)/dV curve for a chain of: (a) 4 sites have peaks ranging from *2.86180508μS* to *2.86180542μS*; (b) 6 sites have peaks ranging from *4.27504215μS* to *4.27504265μS*, (c) 8 sites have peaks ranging from *6.3861741μS* to *6.3861748μS* and (d) 10 sites have peaks range from *9.53984035μS* to *9.53984140μS*. All the calculations were done using the same temperature.

Next we adopt $\delta = 0.6$eV for even chain. Figure 8(a) is observed the ausence of the DOS peak at $\varepsilon_F = 0eV$ indicating the emergence of a localized state in Fermi level. Figure 8(b) has a tail and wide bias window where the Fermi level is close to conduction region band [47]. The inset of the Fig. 8(b) shows the range for n = 4, 6 and 8 which can´t be clearly observed in Fig. 8(b).

Preprints (www.preprints.org) | NOT PEER-REVIEWED | Posted: 27 March 2019

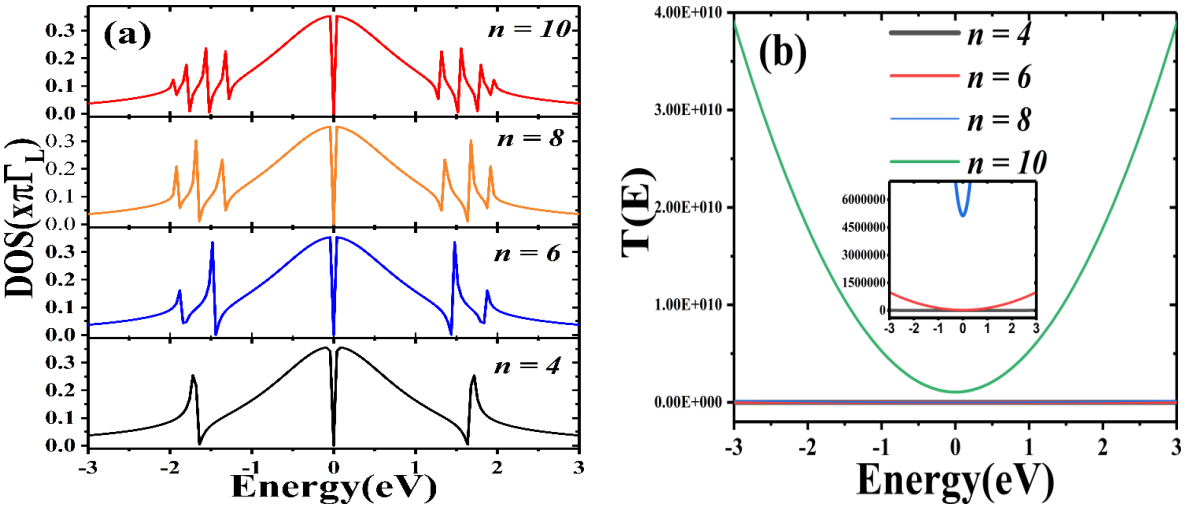

Figure 8. (a) DOS and **(b)** Transmittance [T(E)] versus Energy for the metal/trans-PA/metal system with the coupling parameters $\Gamma_L = \Gamma_R = 0.5$eV; hopping between neighboring sites, in the same subnet, $A = 1+\delta$ and $B = 1-\delta$, where $\delta = 0.6$eV; and chemical potential, $h = 0eV$. **(a)** DOS for even chains (4, 6, 8 and 10 sites) characterizing an energy gap at the Fermi level ($\varepsilon_F = 0$eV) and **(b)** Transmittance for even chains (4, 6, 8 and 10 sites) with a range of $0.e^2/h$ to $4.10^{10}.e^2/h$, in particular, the insert of the **Fig. 8b** ($0.e^2/h$ to $7.10^6.e^2/h$) shows the behavior for 4, 6 and 8 sites.

The *ln(I)-V* curve of the Fig. 9 indicates a small conductivity, although the band theory shows metallic behavior, we identify that the electronic transport is affected by structural and conformational defects, showing the current indicates a semiconductor or insulator behavior.

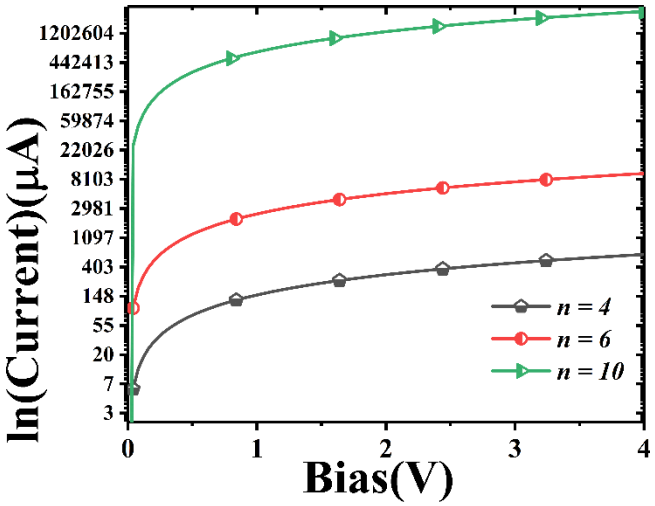

Figure 9. Transport characteristic (ln of the current) from the system coupled to the Leads (Left and Right) to the even chains, (4, 6 and 10 sites) with the paramers $\Gamma = 0.5$eV, hopping $A = 1+\delta$ and $B = 1-\delta$, where $\delta = 0.6$eV.

Similar to Fig. 7 (a-d), we obtained the Fig. 10 (a-d) which presents peaks of the excitation states available in the chain as tunneling paths. Now exhibits oscillations with greater attenuation through the appearance of more quantum wells. The dimer chain for $\delta = 0.6$eV indicates that as the disorder

Preprints (www.preprints.org) | NOT PEER-REVIEWED | Posted: 27 March 2019

increases, states are localized in the center of the band with the transition from localized to delocalized states. Therefore, the electronic transport shows an increase in conductance and indicates a long even chain and an Anderson transition (i. e., are both metal-insulator transitions and quantum-Hall-type transitions between phases with localized states).

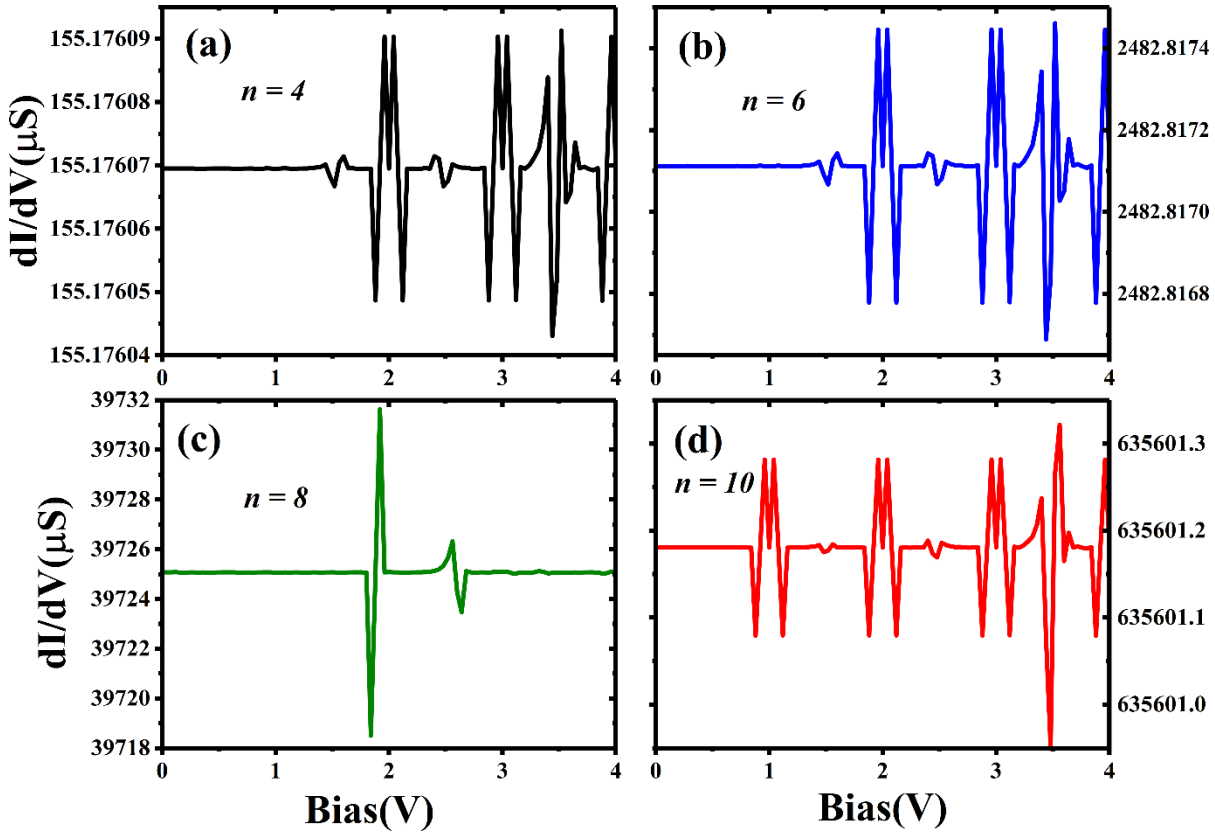

Figure 10. Electronic transport properties (Differential Conductivity) of the system for the even chains (4, 6, 8 and 10 sites) with the parameters $\Gamma = 0.5eV$, hopping $A = 1+\delta$ and $B = 1-\delta$, where $\delta = 0.6$eV for a voltage of $0V$ to $4V$. The $dln(I)/dV$ curves for a chain of: **(a)** 4 sites; **(b)** 6 sites, **(c)** 8 sites and **(d)** 10 sites, all with the same temperature.

In general, starting the metal phase for $\delta = 0.1$eV in the odd chain (i. e., $n = 3, 5, 7$ *and* 9 sites), the system undergoes a metal-insulator transition in the conductivity at $0.5V$ going from metal to semiconductor. For the even chains (i. e., $n = 4, 6, 8$ *and* 10 sites) have: (*i*) the insulating phase to $\delta =$ 0.1eV, the system undergoes an insulator-metal transition in the conductivity with increase in the *I-V* curve; (*ii*) for $\delta = 0.6eV$, the system undergoes a metal-insulator transition in conductivity from metal to semiconductor with increase of anti-resonance in the conductance curves. The results obtained by means of analytical calculations show peculiar differences between even-odd parity chain in T-shaped device, once the topology dimerization strength.

4. Conclusions

We have analyzed the electronic transport characteristics in odd-even dimerized trans-PA molecules coupled to metallic Leads (Left and Right) in the T-shaped geometry based on SSH model. Our analytical calculations used the Heisenberg´s equation of motion technique and the Keldysh´s formalism to obtain the Green´s functions. It has side found that for odd number of sites (i. e., 1, 3 and 5 sites) presenting non-linear (or non-ohmic) behavior similar to electronic device called FET. In addition to the investigation of zero energy states that exhibit a nontrivial topology with prominence

Preprints (www.preprints.org) | NOT PEER-REVIEWED | Posted: 27 March 2019

for even chains and we control electronic tune through different dimerization strength (δ) of chain and analyze for all driving windows -4.0V to 4.0 V.

Controlled by δ a non trivial process of conductance is observed once for even number of sites (i. e., n = 2, 4, 6, 8 and 10) show a odd-even parity effect. In fact, this corroborates in identifying how the electron can be transferred in the device either by coherent transport or by electron scattering, though the transport properties are determined directly by the nature of the electronic structure, the structure of the electronic system is decided by the geometry of the system, so these two factors are interactional.

Based on a more realistic model of 1-D chains, our results are in agreement with the literature. This procedure shows an analytical and numerical study in systems with parameters that are accessible experimentally. Therefore, it can be applied to systems such as Condensed Matter / Cold Atom [48, 49] which have been proposed as semiconductor wires with states localized via a defect in the chain. In addition, our results show that Trans-PA is a sensor that differentiates between even and odd chains of conjugated organic polymers.

Acknowledgments: This work was partially supported by the Brazilian agencies CNPq, CAPES, PROPESP/UFPa and PIBIC/UFPa.

Author Contributions: For research articles with several authors, Jorsi J. da C. Cunha, Miraci S. Costa, Antonio T. M. Beirão and Shirsley S. da Silva performed the calculations. Jorsi J. da C. Cunha, Shirsley S. da Silva, Carlos A. B. da Silva Jr. and Jordan Del Nero discussed and analyzed the data and made the interpretation of the results. Shirsley S. da Silva, Carlos A. B. da Silva Jr. and Jordan Del Nero wrote the paper and made the paper revision.

Conflicts of Interest: The authors declare no conflict of interest.

References

[1] McCreery, R.L. Molecular Electronic Junctions. *Chem. Mater* **2004**, 16, 4477-4496. https://doi.org/10.1021/cm049517q

[2] Del Nero, J. and Laks, B. Effect of Bipolaron type of defect on the polyacetylene-polycarbonitrile copolymer. *Synth. Met*. **1997**, 84, 869-870. https://doi.org/10.1016/S0379-6779(96)04187-2.

[3] Friend *et al*., R.H. Electronic properties of conjugated polymers. *Phil. Trans. R. Soc. Lond. A* **1985**, 314, 37-49.

[4] Su, W.P.; Schrieffer, J. R. and Heeger, A. J. Soliton excitations in polyacetylene. *Phys. Rev. B* **1980**, 22, 2099-2111. https://doi.org/10.1103/PhysRevB.22.2099

[5] Heeger, A.J.; Kivelson, S.; Schrieffer, J.R. and Su, W.P. Solitons in conducting polymers, *Rev. Mod. Phys*. **1988**, 60, 781-850. https://doi.org/10.1103/RevModPhys.60.781

[6] Wei, J.H.; Liu, X.J.; Xie, S.J. and Yan, Y.J. Spin-dependent current modulation in organic spintronics. *J. Chem. Phys*. **2009**, 131, 0649061 (1-5). https://doi.org/10.1063/1.3206737.

[7] Ashhadi, M. and Ketabi, S.A. Tunnel magnetoresistance of FM–organic molecule–FM junction: A Green's function approach. *Physica E: Low-dimensional Systems and Nanostructures* **2001**, 43, 208-1212. https://doi.org/10.1016/j.physe.2011.02.001.

[8] VahediFakhrabad, D.; Shahtahmassebi, N.; Askari, M.; Ashhadi, M. and Ketabi, S.A. Tunnel magnetoresistance of the system of ferromagnetic electrode/polyacetylene/ferromagnetic electrode: A Green's function approach. *Physica E*: *Low-dimensional Systems and Nanostructures* ***2010***, 43, 620-624. https://doi.org/10.1016/j.physe.2010.10.008

Preprints (www.preprints.org) | NOT PEER-REVIEWED | Posted: 27 March 2019

[9] Modarresi, M.; Roknabadi, M.R.; Shahtahmasbi, N.; Vahedi, D. and Arabshahi, H. Evaluation of electronic and transport properties of a nano-scale device in the presence of electric field. *Physica E*: *Low-dimensional Systems and Nanostructures* **2010**, 43, 402-404. https://doi.org/10.1016/j.physe.2010.08.021.

[10] Saitner*et al*., M. Impact of Functional Groups onto the Electronic Structure of Metal Electrodes in Molecular Junctions. *J. Phys. Chem. C* **2012**, 116, 21810-21815. https://doi.org/10.1021/p.3059596

[11] Kushmerick*et al.*, J.G. Understanding Charge Transport in Molecular Electronics. *Ann. N. Y. Acad. Sci.* **2004**, 1006, 277-290. https://doi.org/10.1196/annals.1292.019

[12] Nakayama, H. and Kimura, S. Oligo(phenyleneethynylene) as a molecular lead for STM measurement of single molecule conductance of a helical peptide. *Chem. Phys. Lett.* **2011**, 508**,** 281-284. https://doi.org/10.1016/j.cplett.2011.04.063

[13] Beirão *et al*., A.T.M. Majorana bound states in a quantum dot device coupled with a superconductor zigzag chain. *J. Comput. Electron.* **2018**, 17, 959-966. https://doi.org/10.1007/s10825-018-1206-9

[14] Su, W.P.; Schrieffer, J.R. and Heeger, A.J. Solitons in Polyaeetylene. *Phys. Rev. Lett.* **1979**, 42, 1698-1701. https://doi.org/10.1103/PhysRevLett.42.1698

[15] Li, M. and Lin, X. Adapted Su-Schrieffer-Heeger Hamiltonian for polypyrrole. *Phys. Rev. B* **2010**, 82, 155141 (1-8). https://doi.org/10.1103/PhysRevB.82.155141

[16] Marque, A.M. and Dias, R.G. Multihole edge states in Su-Schrieffer-Heeger chains with interactions. *Phys. Rev. B* **2017**, 95, 115443 (1-7). https://doi.org/10.1103/PhysRevB.95.115443

[17] Anderson, P.W. The question of classical localization A theory of white paint? *Philos. Mag. B* **1985**, 52, 505-509. https://doi.org/10.1080/13642818508240619

[18] Mott, N.F. Metal-Insolatortransintion, Taylor& Francis, London. *Cryst. Res. Technol.* **1990**, 26, 788-788. https://doi.org/10.1002/crat.2170260620

[19] Hubbard, J. Electron correlations in narrow energy bands. *Proc. R. Soc. A* **1963**, 276, 238-257.

[20] Hubbard, J. Electron correlations in narrow energy bands-II- The degenerate band case. *Proc. R. Soc. A* **1964**, 277, 237-259. https://doi.org/10.1098/rspa.1964.0019

[21] Anderson, P.W. Localized Magnetic States in Metals. *Phys, Rev.* **1961**, 124**,** 41-56. https://doi.org/10.1103/PhysRev.124.41

[22] Mouruk, V.; Zuo, K.; Frolov, S.M.; Plissard, S.R.; Bakkers, E.P.A.M. and Kouwernhoven, L.P. Signatures of Majorana Fermions in Hybrid Superconductor-Semiconductor Nanowire Devices. *Science* **2012**, 336**,** 1003-1007. https://doi.org/10.1126/science.1222360

[23] León, I.; Yang, Z. and Wang, L.-S. Probing the electronic structure and Au–C chemical bonding in $AuC_2^-$and AuC_2 using high-resolution photoelectron spectroscopy. *J. Chem. Phys.* **2014**, 140, 084303(1-13). https://doi.org/10.1063/1.4865978

[24] Dai, X.; Zhang, L.; Li, J.; Wang, Z. and Li, H. Electronic transport properties of heterojunction devices constructed by single-wall Fe_2Si and carbon nanotubes. *J. Mater. Chem. C* **2018,** 6, 5794-5802. https://doi.org/10.1039/C8TC01708E

[25] Lissel, F.; Schwarz, F.; Blacque, O.; Riel, H.; Lörtscher, E.; Venkatesan, K. and Berke, H. Organometallic Single-Molecule Electronics: Tuning Electron Transport through X(diphosphine)$_2$FeC$_4$Fe(diphosphine)$_2$X Building Blocks by Varying the Fe–X–Au Anchoring Scheme from Coodinative to Covalent. *J. Am. Chem. Soc.* **2014**, 136**,** 14560-14569. https://doi.org/10.1021/ja507672g

[26] Keldysh, L.V. Diagram technique for nonequilibrium processes, *Sov. Phys. JETP* **1965**, 20, 1018-1026.

[27] Galperin, M.; Ratner, M.A. and Nitzan, A. Molecular transport junctions: vibrational effects. *J. Phys. Condens. Matter* **2007**, 19, 103201(1-81). https://doi.org/10.1088/0953-8984/19/10/103201

Preprints (www.preprints.org) | NOT PEER-REVIEWED | Posted: 27 March 2019

[28] Koch, T.; Loos, J.; Alvermann, A. and Fehske, H. Nonequilibrium transport through molecular junctions in the quantum regime.*Phys. Rev.* B **2011**, 84, 125131 (1-16). https://doi.org/10.1103/PhysRevB.84.125131

[29] Koch, T.; Fehske, H. and Loos, J. Phonon-affected steady-state transport through molecular quantum dots, *Phys. Scr.* **2012**, T151, 014039 (1-10). https://doi.org/10.1088/0031-8949/2012/T151/014039

[30] Wei, J.H.; Xie, S.J.; Mei, L.M.; Berakdar, J. and Yan, Y.J. Charge-transfer polaron induced negative differential resistance and giant magnetoresistance in organic spin-valve systems. *New J. Phys*. **2005**, 8, 82 (1-9). https://doi.org/10.1088/1367-2630/8/5/082

[31] Wei, J.H.; Xie, S.J.; Mei, L.M.; Berakdar, J. and Yan, Y.J. Conductance switching, hysteresis, and magnetoresistance in organic semiconductors. *Org. Electron.* **2007**, 8, 487-497. https://doi.org/10.1016/j.orgel.2007.03.002

[32] Sun, X.; Fu, R.L.; Yonemitsu, K. and Nasu, K. Photoinduced Polarization Inversion in a Polymeric Molecule. *Phys. Rev. Lett*. **2000**, 84, 2830-2832. https://doi.org/10.1103/PhysRevLett.84.2830

[33] Sun, X.; Fu, R.L.; Yonemitsu, K. and Nasu, K. Photoinduced phenomenon in polymers. *Phys. Rev. A* **2001**, 64, 032504 (1-7)A. https://doi.org/10.1103/PhysRevA.64.032504.

[34] Bruus, H. and Flensberg, K. Many-Body Quantum Theory in Condensed Matter Physics, Oxford University Press, New York, USA, **2006**, 466-466.

[35] Shen, S.-Q. Topological Insulators, Dirac Equation in Condensed Matters (Springer Series in Solid-State Science 174, Berlin,Germany, **2012**, pp 225-225).

[36] Xiong, Y. and Tong, P. A NOT operation on Majoranaqubits with mobilizable solitons in an extended Su–Schrieffer–Heeger model, *New J. Phys*. **2015**, 17, 013017 (1-10). https://doi.org/10.1088/1367-2630/17/1/013017.

[37] Haug, H. and Jauho, A.-P. Quantum Kinetics in Transport and Optics of Semiconductors (Springer Series in Solid-State Sciences **123**, Second Edition, 2008, pp 339-339).

[38] Do, V.N. Non-equilibrium Green function method: theory and application in simulation of nanometer electronic devices. *Adv. Nat. Sci. Nanosci. Nanotechnol*. **2014**, 5, 033001 (1-21) https://doi.org/10.1088/2043-6262/5/3/033001.

[39] Kraus, C.V.; Diehl, S.; Zoller P. and Baranov, M.A. Preparing and probing atomic Majorana fermions and topological order in optical lattices. *New J. Phys.* **2012**, 14**,** 113036 (1-17). https://doi.org/10.1088/1367-2630/14/11/113036

[40] Law, K.T.; Lee P.A. and Ng, T.K. Majorana fermion induced resonant Andreev reflection. Phys. Rev. Lett. **2009**, 103**,** 237001 (1-4). https://doi.org/10.1103/physrevlett.103.237001

[41] Aleixo, V.F.P.; Silva Jr., C.A.B. and Del Nero, J. Electronic transport in cyclic carotenoids based π conjugation system.*Sci. Adv. Today* **2016**, 2, 25258 (1-6).

[42] Horiguchi, K.; Tsutsui, M.; Kurokawa, S. and Sakai, A. Electron transmission characteristics of Au/1,4-benzenedithiol/Au junctions. *Nanotechnology* **2009**, 20, pp 025204 (1-7). https://doi.org/10.1088/0957-4484/20/2/025204.

[43] Oliveira, A.S.; Beirão, A.T. M.; Silva, S.J.S. and Del Nero, J. Electronic signature of single-molecular device based on polyacetylene derivative, *J. Comput. Electron.* **2018**, 17, 586-594. https://doi.org/10.1007/s10825-018-1160-6

[44] Larade, B.; Taylor, J.; Mehrez, H. and Guo, H. Conductance, I-V curves, and negative differential resistance of carbon atomic wires, *Phys. Rev. B* **2001**, **64**, 075420 (1-10). https://doi.org/10.1103/PhysRevB.64.075420

[45] Khoo, K.H.; Neaton, J.B.; Son, Y.W.; Cohen, M.L. and Louie, S.G. Negative differential resistance in carbon atomic wire-carbon nanotube junction, *Nano Lett.* **2008**, 8, 2900-2905. https://doi.org/10.1021 / nl8017143

Preprints (www.preprints.org) | NOT PEER-REVIEWED | Posted: 27 March 2019

[46] Ashhadi, M.; Ketabi, S.A.; Shahtahmasebi, N.; VahediFakhrabad, D. and Askari, M. The role of impurities on the properties of electron transport through the metal/trans-PA/metal system: Green's function approach. *Physica E: Low-dimensional Systems and Nanostructures* **2011**, 43, 924-928. https://doi.org/10.1016/j.physe.2010.11.015

[47] Wang, L.; Ling, W.; Zhang, L. and Xiang, D. Advance of Mechanically Controllable Break Junction for Molecular Electronics. *Top. Curr. Chem.* **2017**, 375, 61-68. https://doi.org/10.1007/s41061-017-0149-0

[48] Jiang, et al., L. Majorana fermions in equilibrium and in driven cold-atom quantum wires. *Phys. Rev. Lett.* **2011**, 106, 200402 (1-4). https://doi.org/ 10.1103/physrevlett.106.220402

[49] Zhang, C.; Tewari, S.; Lutchyn, R.M. and Sarma, S. *px+ ipy* Superfluid from s-wave interactions of Fermionic cold atoms. *Phys. Rev. Lett.* **2008**, 101, 160401 (1-4). https://doi.org/10.1103/physrevlett.101.160401.